

Geophysical Research Letters

RESEARCH LETTER

10.1002/2014GL060139

Key Points:

- Spatially coherent and significant deformation transients in the Tohoku region
- Transients in south-central Tohoku cannot be explained by afterslip
- Increasing slip rate and updip migration of deep slip before the M 9 Tohoku event

Supporting Information:

- Readme
- Figure S1
- Figure S2
- Figure S3
- Figure S4
- Figure S5
- Figure S6
- Figure S7
- Figure S8
- Figure S9
- Figure S10
- Figure S11
- Figure S12
- Text S1
- Table S1
- Table S2
- Table S3

Correspondence to:

A. P. Mavrommatis,
andreas.m@stanford.edu

Citation:

Mavrommatis, A. P., P. Segall, and K. M. Johnson (2014), A decadal-scale deformation transient prior to the 2011 M_w 9.0 Tohoku-oki earthquake, *Geophys. Res. Lett.*, 41, 4486–4494, doi:10.1002/2014GL060139.

Received 9 APR 2014

Accepted 25 JUN 2014

Accepted article online 27 JUN 2014

Published online 15 JUL 2014

A decadal-scale deformation transient prior to the 2011 M_w 9.0 Tohoku-oki earthquake

Andreas P. Mavrommatis¹, Paul Segall¹, and Kaj M. Johnson²

¹Department of Geophysics, Stanford University, Stanford, California, USA, ²Department of Geological Sciences, Indiana University, Bloomington, Indiana, USA

Abstract GPS time series in northeast Japan exhibit nonlinear trends from 1996 to 2011 before the M_w 9.0, 2011 Tohoku-oki earthquake. After removing reference frame noise, we model time series as linear trends plus constant acceleration, correcting for coseismic and postseismic effects from the numerous $M_w \sim 6.5+$ earthquakes during this period. We find spatially coherent and statistically significant accelerations throughout northern Honshu. Large areas of Japan outside the Tohoku region show insignificant accelerations, demonstrating that the observation is not due to network-wide artifacts. While the accelerations in northern Tohoku (Sanriku area) can be explained by decaying postseismic deformation from pre-1996 earthquakes, the accelerations in south-central Tohoku appear unrelated to postseismic effects. The latter accelerations are associated with a decrease in average trench-normal strain rate and can be explained by increasing slip rate on the Japan trench plate interface and/or updip migration of deep aseismic slip in the decades before the 2011 Tohoku-oki earthquake.

1. Introduction

The northeastern Japan subduction zone accommodates ~ 83 mm/yr of relative motion between the Pacific and North American plates [DeMets *et al.*, 2010]. Average interseismic GPS velocities in northern Honshu reveal contraction perpendicular to the Japan trench (Figure 1a), consistent with significant coupling on the plate interface [Nishimura *et al.*, 2004; Hashimoto *et al.*, 2009; Loveless and Meade, 2010]. The decade preceding the M_w 9.0 11 March 2011 Tohoku-oki earthquake was marked by a sequence of $M_w \geq 6.5$ interplate earthquakes, with a pronounced increase in activity after 2003 (no $M_w \geq 6.5$ seismicity during the period 1997–2003 versus five interplate events in the period 2003–2011). These events were followed by unusually large postseismic transients, with displacements as large as or larger than their corresponding coseismic displacements [Suito *et al.*, 2011].

Recent studies have reported that the GPS-inferred rate of deformation in the south-central Tohoku region decreased in the period 2003–2011 relative to 1997–2003, with the latter period assumed to represent steady state [Geospatial Information Authority of Japan, 2011; Ozawa *et al.*, 2012; Nishimura, 2012; Heki and Mitsui, 2013]. This change has been interpreted as decrease in the coupling of the plate interface after 2003, due to the copious afterslip following the interplate earthquakes [Ozawa *et al.*, 2012; Heki and Mitsui, 2013]. However, it remains unclear whether afterslip was the sole source of the observed change in the deformation rate, or whether the data also require an additional, longer-duration (decadal-scale) transient that may extend back prior to 2003. In addition, previous studies did not account for possible “ghost transients” from large earthquakes prior to 1997, which could have significant effects on contemporary deformation rates [e.g., Hearn *et al.*, 2013].

In the absence of postseismic transients and episodic slow-slip events [Peng and Gomberg, 2010], interseismic deformation is observed to accumulate at a steady rate [e.g., Anderson *et al.*, 2003; Rolandone *et al.*, 2008]. Thus, it is essential to correct for well-understood transients before interpreting any apparent decadal-scale change in deformation rate, especially given the apparent spatial and temporal association with the M_w 9.0, 2011 Tohoku-oki earthquake. In this study, we remove transient postseismic effects from all moderate and large earthquakes that could influence the GPS time series. We quantify the residual time rate of change in GPS velocities, thereby producing a map of interseismic crustal accelerations. We then investigate the implications of the estimated accelerations in terms of temporal behavior of the coupling on the plate interface.

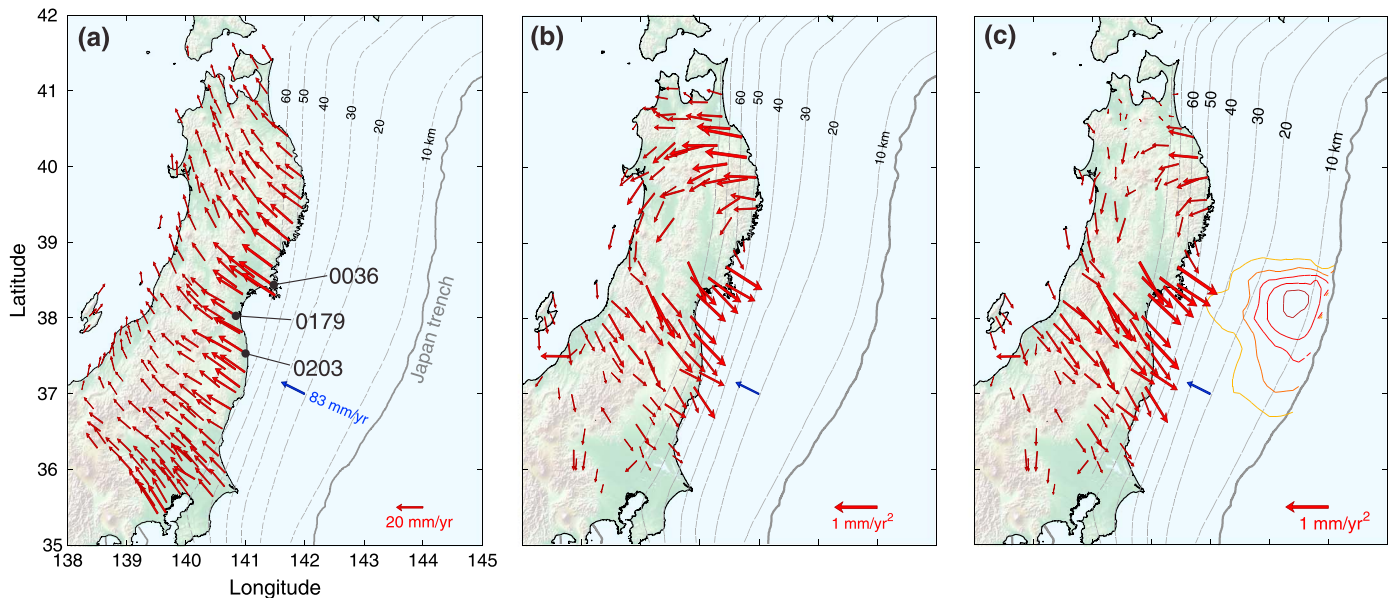


Figure 1. (a) Instantaneous velocity field in northern Honshu, Japan in 2003, in a stable North America reference frame (red vectors). Blue vector shows the convergence direction between the Pacific and North American plates from DeMets et al. [2010]. Isodepth contours of the plate interface from Baba et al. [2006] are shown as dashed lines. (b) Estimated acceleration field for the period 1996 to 2011 (red vectors). Stations with an RMS misfit larger than 4 mm and an acceleration signal-to-noise ratio (SNR) smaller than 1 are omitted. See Figure S6 in the supporting information for a version in which accelerations are colored by SNR. (c) Residual acceleration field after removing modeled accelerations due to postseismic viscoelastic effects of large earthquakes before 1996. Contours indicate the slip distribution of the 2011 M_w 9.0 Tohoku-oki earthquake in 10 m intervals [Hooper et al., 2013].

2. Data and Methods

We analyze horizontal position time series from 891 GEONET stations throughout Japan with at least 10 years of data in the period 21 March 1996 to 6 February 2011. Data are from the GEONET F3 solution published by the Geospatial Information Authority of Japan [Nakagawa et al., 2009]. First, we verify that the apparent rate change is not present in all GEONET stations (Figure S1 in the supporting information), which could indicate a reference frame drift. We remove common-mode errors by subtracting daily rigid body translations and rotations from all time series, estimated from a set of reference stations around Japan (Text S1 and Figures S2 and S3). We estimate errors in the daily positions, assumed to be the sum of white and time-dependent noise, using maximum-likelihood methods from selected time series that are well fit by a linear trend, as in Langbein [2004]. We find a white-noise amplitude of 1.5 mm and time-dependent noise spectral index of $n = 1.5$ with amplitude of $3.4 \text{ mm/yr}^{n/4}$.

We model the position time series as a superposition of four types of signal: (1) interseismic deformation, (2) seasonal signal, (3) nontectonic offsets (e.g., GPS antenna changes), and (4) coseismic offsets and postseismic transients caused by $M_w \geq 6.3$ earthquakes in the time period 1996 to 2011. Inspection of raw time series reveals that many exhibit obvious curvature; i.e., increasing deviations from an initial rate (Figures 2 and S1). To quantify this curvature, we add constant acceleration, a , to the standard linear model, such that $x(t) = x_0 + v_0 t + \frac{1}{2} a t^2$, where x_0, v_0 are initial position and velocity, recognizing that this is a first-order representation of actual long-duration transients. The model equation for each component of the time series is thus

$$x(t) = x_0 + v_0 t + \frac{1}{2} a t^2 + \sum_{m=1}^2 [S_m \sin(m\omega t) + C_m \cos(m\omega t)] + \\ + \sum_{j=1}^{N_{\text{off}}} O_j H(t - t_j^{\text{off}}) + \sum_{i=1}^{N_{\text{eq}}} [A_i + B_i f(t - t_i^{\text{eq}})] H(t - t_i^{\text{eq}}). \quad (1)$$

Here $\omega = 2\pi/T$ with T equal to one year, N_{off} is the number of nontectonic offsets, $H(t)$ is a Heaviside step function, N_{eq} is the number of earthquakes included in the analysis, and A_i and $B_i f(t - t_i^{\text{eq}})$ are coseismic offsets and postseismic transients following each earthquake, respectively, with $f(t)$ being the time dependence of the postseismic transient.

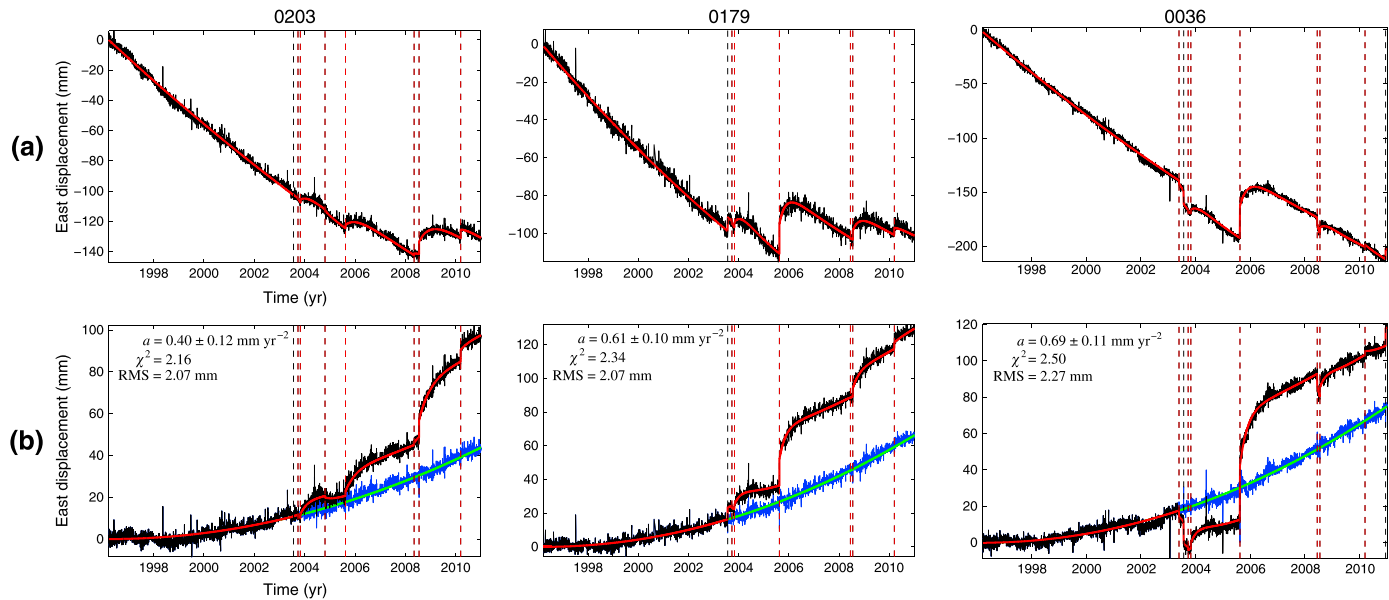


Figure 2. Representative GPS position time series from south-central Tohoku. (a) East component time series after removing common-mode errors (black curves) and model fits (red curves) from stations 0203, 0179, and 0036, respectively (locations in Figure 1). Vertical dashed lines mark times of detected antenna offsets (black) and earthquakes (red). (b) As in Figure 2a but with initial linear trends removed (black and red), as well as with offsets and postseismic transients removed (blue and green).

Removing the effects of earthquakes in the time series (i.e., detecting coseismic offsets and postseismic transients) is not trivial, for two reasons. First, because earthquakes between 2003 and 2011 were close in space and time, separating the effects of individual events is difficult. Second, several time series exhibit obvious postseismic transients without detectable coseismic offsets; therefore, assigning postseismic transients only when a coseismic offset is detected results in an underestimation of the postseismic deformation.

To overcome these issues, we must take into account the spatial pattern of postseismic deformation. We make the simplifying assumption that postseismic displacements can be written in the form

$\mathbf{u}(\mathbf{x}, t) = \mathbf{U}(\mathbf{x})f(t)$, where $\mathbf{U}(\mathbf{x})$ is a spatial basis and $f(t) \rightarrow 1$ as $t \rightarrow \infty$. This formulation assumes there is little temporal change in the spatial distribution of afterslip, consistent with some geodetic inversions [e.g., Fukuda *et al.*, 2013]. The procedure is (1) use a physical model to form spatial bases for coseismic and cumulative postseismic displacements, $\mathbf{U}(\mathbf{x})$, for each earthquake; (2) fit the observed GPS displacements and define the area of influence of each earthquake; (3) fit individual time series using equation (1), including terms for an earthquake's offset and transient only if the station is located inside the estimated area of influence of that earthquake.

We employ the subduction interface geometry of Baba *et al.* [2006] and represent the seven $M_w \geq 6.3$ interplate earthquakes that occurred in the period 2003 to 2011 as circular cracks of 20 km radius (Table S1 and Figure S4). Each crack undergoes uniform shear stress drop at the time of the earthquake. For each earthquake, we compute the cumulative afterslip distribution that fully relaxes the coseismic stress change outside the crack; afterslip is restricted to occur outside predefined source regions (seismic asperities), as in Johnson *et al.* [2012] (Text S1). We then compute coseismic and fully relaxed postseismic displacement bases (for unit stress drop), $\mathbf{U}(\mathbf{x})$, using homogeneous elastic Green's functions. For earthquakes that did not occur on the Japan trench, we compute displacement bases assuming uniform coseismic and fully relaxed postseismic slip on rectangular faults, the geometry of which is constrained from published parameters (Table S2).

The temporal evolution of afterslip, $f(t)$, is taken from the displacement response, $\delta(t)$, of a steady state, rate-strengthening spring-slider to a stress step $\Delta\tau$, including load-point velocity v^∞ ,

$$\delta(t) = \frac{\sigma(a - b)}{k} \ln \left[\frac{V_{\max}}{v^\infty} (e^{t/t_c} - 1) + 1 \right] - v^\infty t \quad (2)$$

[*Perfettini and Avouac, 2004*], where σ is normal stress, a and b are the rate-dependent and state-dependent frictional parameters, respectively, k is the spring stiffness, $v_{\max} = v^\infty \exp[\Delta \tau / \sigma(a - b)]$, and $t_c = \sigma(a - b) / kv^\infty$ (details in Text S1).

For each earthquake, we fit the predicted coseismic and cumulative postseismic displacements to the GPS data by adjusting the coseismic stress drop (or slip magnitudes, for non-Japan Trench earthquakes) and the afterslip time constant, t_c . The area of influence for each earthquake is taken to be where the fully relaxed postseismic displacements exceed 3 mm (about 2x the data noise level). The time series model (equation (1)) includes terms for a given earthquake only if the station is located inside that earthquake's area of influence. This criterion avoids overparameterization, by modeling only the earthquakes that produce observable signals in the time series. Model parameters and (co)variances are estimated using standard nonlinear least squares, independently for each station (Text S1). The simple model fits the observed postseismic deformation quite well, both in terms of spatial patterns and time dependence (Figure 3).

Our stress-driven, basis-function method of modeling postseismic deformation is able to separate postseismic effects of earthquakes that are clustered in space and time, such as the 2008.4 Ibaraki and 2008.6 Fukushima events (Figure 3h). In contrast, *Suito et al. [2011]*, who performed regularized (smoothed) kinematic slip inversions for different time intervals, inferred that postseismic moment from the 2008.6 earthquake was more than 3.5 times the coseismic moment, recognizing that much of this postseismic moment likely resulted from the 2008.4 event. Indeed, Figure 3e shows that much of the afterslip distribution after the 2008.6 event is attributed to continued afterslip from the 2008.4 event. Continued afterslip from previous events can also be seen in other periods (e.g., Figure 3c and 3f).

3. Results and Interpretations

The fit to the time series is reasonable, with a mean reduced chi-square statistic of $\chi^2_v = 2.92$. Removing linear trends, offsets, and postseismic transients from the time series reveals that stations in this region exhibit accelerating motion in the period 1996 to 2011 (Figure 2). The estimated acceleration field in northern Honshu is shown in Figure 1b. In addition to being statistically significant (on average 3.2σ , equivalent to 99.9% confidence), the accelerations are spatially coherent. We observe landward accelerations in northern Tohoku (latitudes 39° – 41°) and trenchward accelerations in central and southern Tohoku (latitudes 36.5° – 39°). In contrast, large areas of Japan exhibit insignificant accelerations (Figure S7), demonstrating that accelerations in the Tohoku region are not due to network-wide artifacts.

The landward acceleration in northern Tohoku likely results from continued postseismic deformation following the 1994 $M_w 7.7$ Sanriku-oki earthquake, which occurred just over a year prior to the beginning of the GPS time series. In fact, deformation in this region can be modeled as postseismic transients of the form $x(t) = x_0 + vt + Bf(t - t^{eq})$ (Figure S8).

Postseismic deformation also results from flow in the lower crust and upper mantle. Such transients can last as long as several decades [*Thatcher, 1983*] and large historic earthquakes can perturb contemporary GPS velocity fields [*Hearn et al., 2013*, and references therein]. Northeastern Japan experienced several $M_w \sim 7$ – 8 earthquakes in the decades before the 2011 Tohoku earthquake. We therefore test to what extent the observed accelerations can be explained by ghost transients due to earthquakes prior to 1996, assuming that viscoelastic effects dominate afterslip at long times since the earthquakes. We compute accelerations due to viscoelastic effects of $M_w \geq 7.5$ earthquakes in northeastern Japan that occurred in the period 1938–1996 using published estimates of source parameters, including approximate fault geometry and moment magnitude (Text S1, Table S3, and Figure S9).

For events on the Japan Trench (e.g., 1968 $M_w 8.3$ and 1994 $M_w 7.7$ Sanriku-oki earthquakes) we find that a viscosity of 10^{19} Pa s and a postseismic moment of 1.5 times the coseismic moment (to account for rapid afterslip) explains much of the GPS-inferred accelerations in the Sanriku area. For events near the Sea of Japan coastline (e.g., 1993 $M_w 7.7$ Hokkaido-Nansei-oki and 1983 $M_w 7.6$ Sea of Japan earthquakes), a viscosity of 10^{18} Pa s is needed to fit to the GPS accelerations in northern Honshu and southwest Hokkaido. This is consistent with *Ueda et al. [2003]*, who inferred a low-viscosity (4×10^{18} Pa s) uppermost mantle in the back-arc side of northeastern Japan analyzing postseismic GPS observations.

Figure 1c shows residual accelerations after subtracting predicted accelerations due to viscoelastic effects from historic earthquakes. We find that about 50% of the landward acceleration in northern Tohoku can

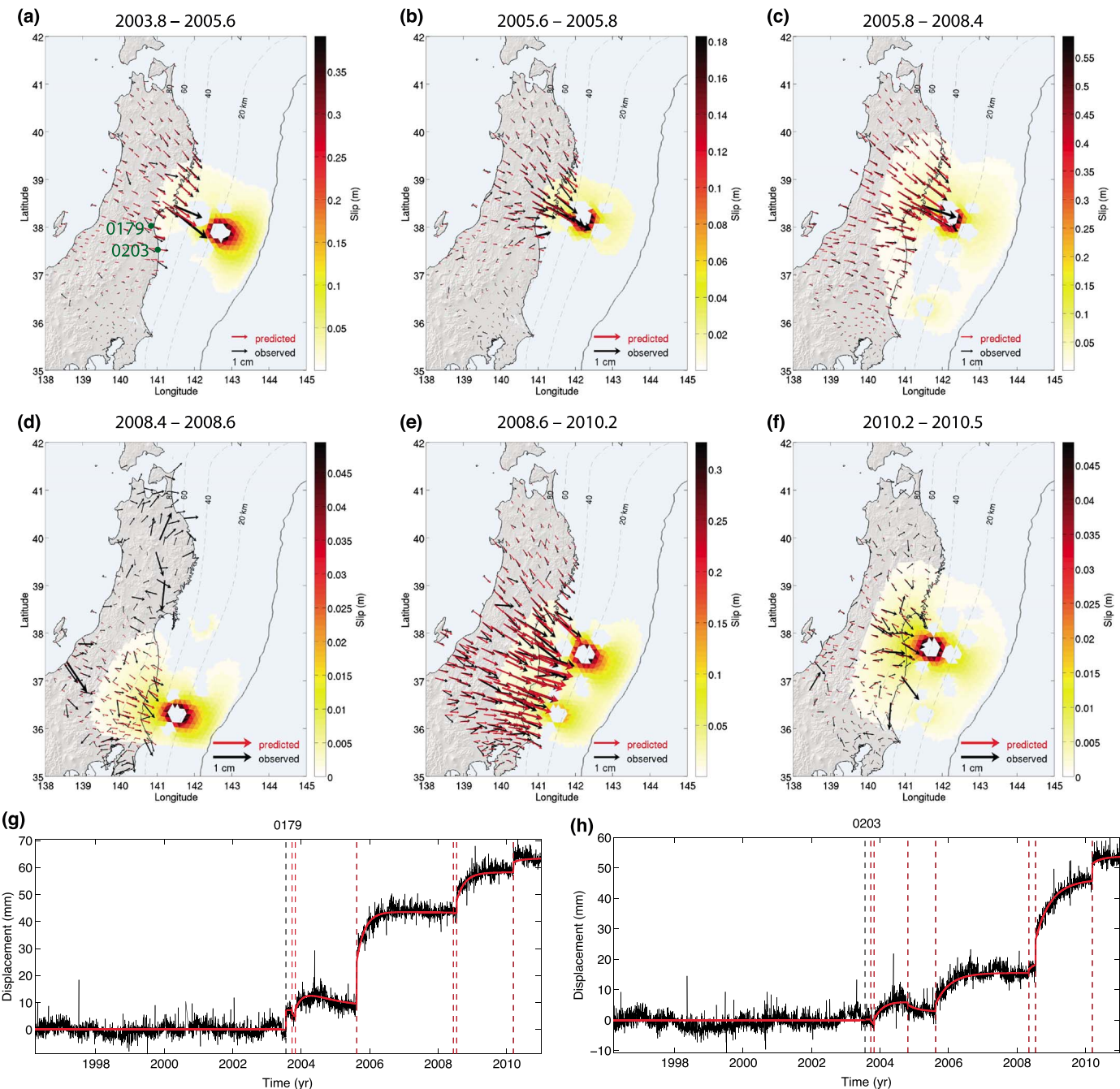


Figure 3. Spatiotemporal fits to postseismic deformation in northeast Japan in the time period 1996–2011. (a–f) Cumulative postseismic displacements (black vectors) for time periods between six interplate earthquakes; red vectors are model fits and colored patches are modeled slip distributions. (Note the change of scale between panels.) (g–h) East-component time series with both linear and quadratic trends removed, from stations 0179 to 0203, respectively; data in black, model fit in red; vertical red lines mark the times of earthquakes that are modeled in each time series; station locations in Figure 3a.

be explained by viscoelastic effects. We suggest that the remaining acceleration in this area could result from sustained afterslip and/or incomplete modeling of viscoelastic effects (Figure S8). In contrast, the trenchward acceleration in south-central Tohoku is much larger than predicted from viscoelastic relaxation. Viscoelastic effects due to the 1964 M_w 7.5 Niigata earthquake produce accelerations with the proper sign (toward the Japan trench); however, their magnitudes are too small and counteracted by effects of the 1938 M_w 8.0 Shioya-oki event. In summary, our modeling suggests that continued postseismic deformation from large pre-1996 earthquakes cannot explain the observed trenchward accelerations in south-central

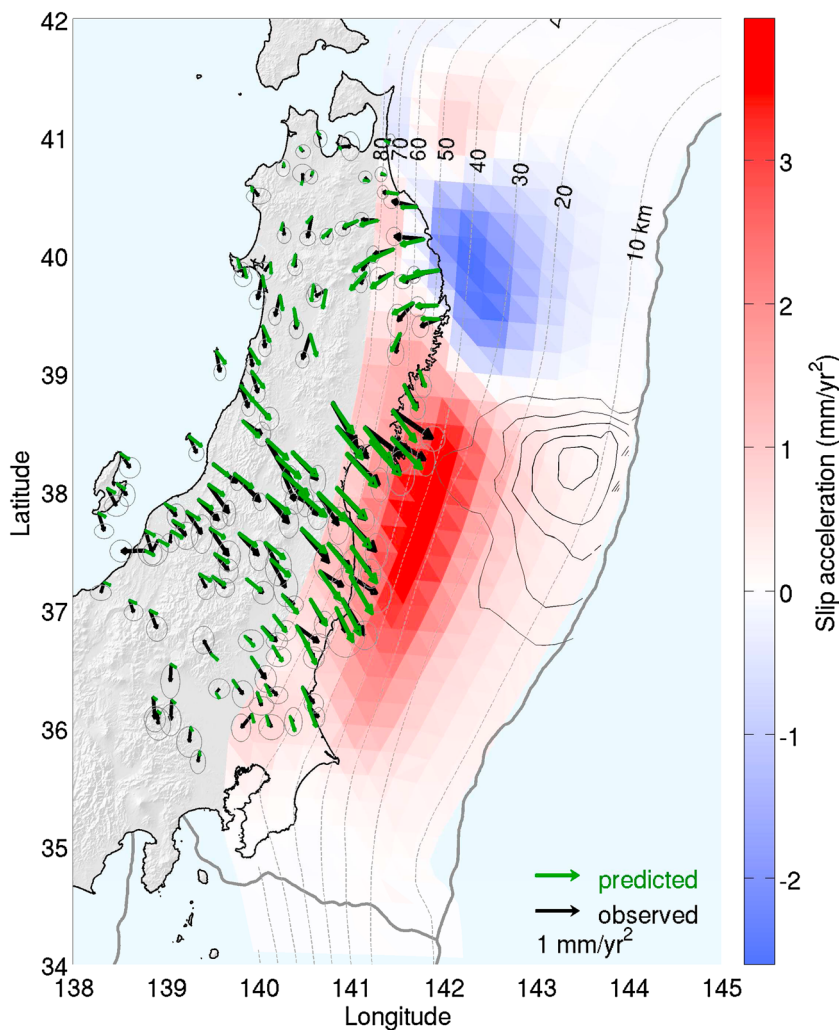


Figure 4. Inversion of interseismic accelerations for slip acceleration on the Japan Trench plate interface. Observed accelerations with 2σ error ellipses are shown in black; model fit in green. Colored patches show the estimated distribution of slip acceleration (dip-slip component) on the plate interface. Black contours indicate the slip distribution of the 2011 M_w 9.0 Tohoku-oki earthquake in 10 m intervals [Hooper et al., 2013].

Tohoku. We also find negligible accelerations in south-central Tohoku due to viscoelastic effects from the 2003 M_w 8.3 Tokachi-oki earthquake (Figure S10).

In south-central Tohoku (latitudes 36.5° to 39°), not only did the magnitude of the interseismic velocity field decrease as a function of time but also its spatial gradient; i.e., strain rate. In a coordinate system aligned with the Japan trench, the average shear strain rate, $\dot{\gamma}_1 = |\dot{\epsilon}_{11} - \dot{\epsilon}_{22}|$ (where $\dot{\epsilon}_{11}$ and $\dot{\epsilon}_{22}$ are average strain rates oriented $N70^\circ W$ and $N20^\circ E$, respectively), decreased by about one third, from $136 \pm 5 \times 10^{-9} \text{ yr}^{-1}$ in 1996 to $106 \pm 2 \times 10^{-9} \text{ yr}^{-1}$ in 2011 (Figure 5a).

Since the change in strain rate in south-central Tohoku cannot be explained by postseismic effects of large historic earthquakes, an additional source of deformation is required. We consider a temporal change in the slip rate on the subduction interface (i.e., time-dependent coupling) as a possible transient deformation source. A regularized (minimum model norm) inversion of the residual acceleration field (corrected for known postseismic effects) for aseismic slip acceleration on the plate interface (Text S1) shows that the residual accelerations can be fit by a ~ 400 km long patch of accelerating creep offshore Tohoku, with predominantly dip-slip motion (Figures 4 and S12). The inversion also predicts a smaller area of decelerating creep offshore northern Tohoku, which we interpret as decaying afterslip from the 1994 Sanriku-oki earthquake, not accounted for in the viscoelastic modeling. Most of the accelerating creep is imaged in the depth range of ~ 20 – 70 km; however, resolution at shallower depths is poor [e.g., Loveless and Meade, 2011].

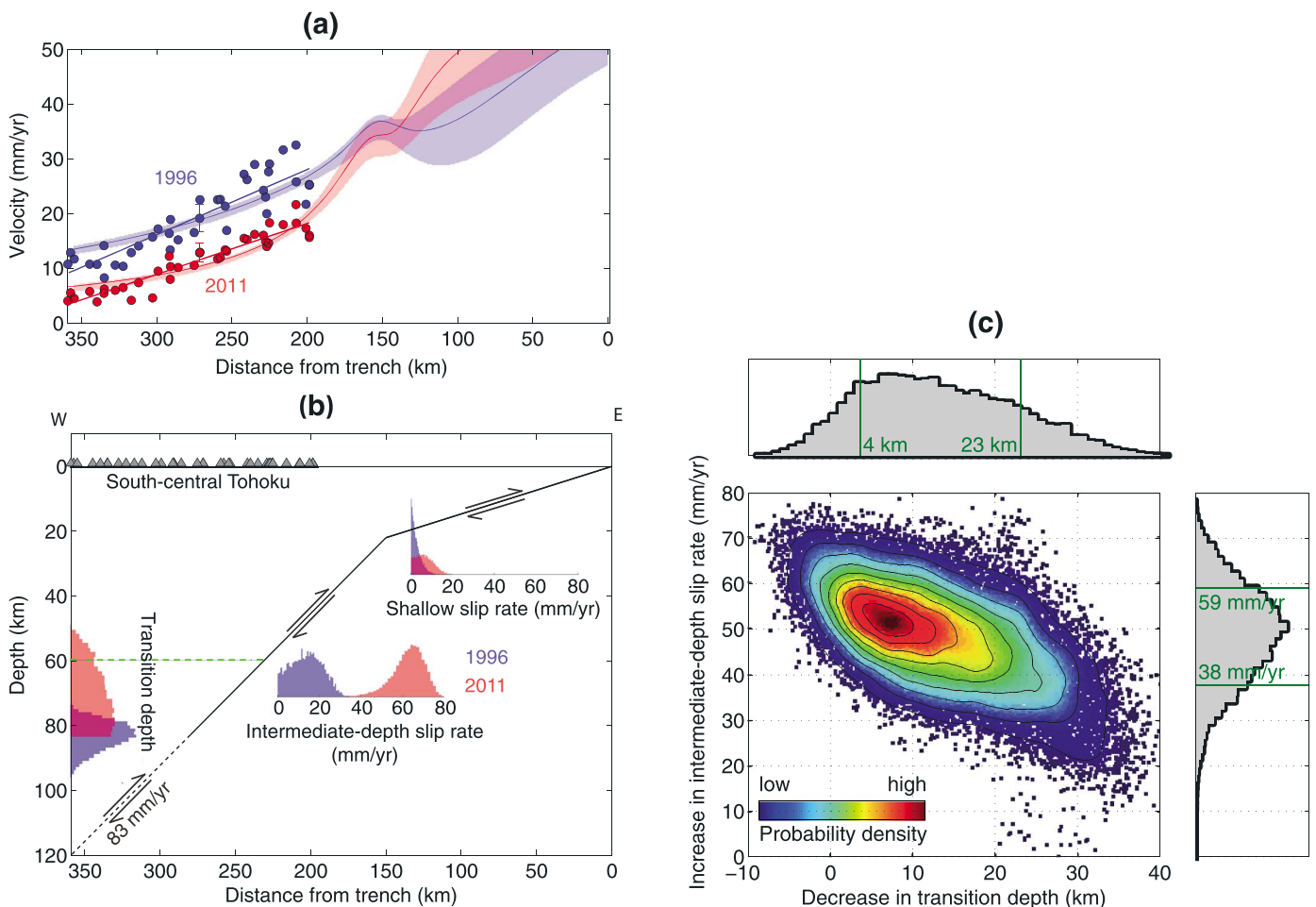


Figure 5. Two-dimensional modeling of change in interseismic velocity in south-central Tohoku (latitudes 36.5° to 39°). (a) Instantaneous velocity field in 1996 (blue) and 2011 (red). Circles are GPS data; representative 1σ error bars are also shown. Straight lines are linear fits. Thin curves are model fits from Bayesian estimation, with shaded regions being 95% confidence bounds. (b) Model geometry for the subduction interface (trench-normal cross section). Gray triangles show station locations. Histograms are estimated posterior probability distributions for the indicated parameters in the two time periods (1996 in blue, 2011 in red). Green dashed line is the approximate downdip limit of seismicity. (c) Correlation between decreasing transition depth and increasing intermediate-depth slip rate from 1996 to 2011. Dots correspond to acceptable models, with warmer colors indicating higher joint probability density. Histograms show marginal posterior probability distributions, with green lines indicating 68% confidence intervals.

The GPS-inferred change in slip rate could be in part due to updip migration of the transition from downdip creep at the full plate rate to a partially locked interface, at a depth we refer to as the “transition depth.” We test this using a simple two-dimensional elastic back slip model of the plate interface, consisting of two segments: a shallow part dipping 8° from the surface to 22 km depth, and a deeper part dipping 25° from 22 km to the transition depth (Figure 5b). We explore the change in the GPS velocities in south-central Tohoku resulting from a combination of change in three parameters: (1) transition depth, (2) slip rate at intermediate depths (between transition depth and 22 km), and (3) slip rate at shallow depths (above 22 km). We conducted a Bayesian estimation using a Markov chain Monte Carlo method for the instantaneous velocities in 1996.4 and 2011.0. We assumed uniform prior distributions on the model parameters, bounding the slip rate between 0 and 83 mm/yr and restricting the transition depth in 2011 to be shallower than the mean value in 1996. Results show that the shallow slip rate was low and did not increase substantially; in contrast, the data are consistent with significant decrease in the transition depth and increase in intermediate-depth slip rate (Figure 5b). The shallowing of the transition depth and increase in intermediate-depth slip rate are anticorrelated (Figure 5c). The most likely decrease in transition depth is in the range of 4 to 23 km, while the increase in intermediate-depth slip rate ranges from 38 to 59 mm/yr (Figure 5c). The latter corresponds to a (spatially averaged) slip acceleration of 2.6 to 4.0 mm/yr² at depths below 22 km, consistent with the 3-D inversion (Figure 4).

4. Discussion

After removing linear trends, coseismic offsets, and postseismic transients, GPS time series from south-central Tohoku reveal an approximately continuous transient spanning the period 1996 to 2011, without any obvious onset (Figure 2). This observation allows for the possibility that the transient began prior to 1996 (the start of the time series). Historic geodetic data from triangulation and trilateration surveys [Hashimoto, 1990; Ishikawa *et al.*, 1998] can provide estimates of average strain rate during the ~100 years before the GPS era and, thus, potentially constrain which part of the GPS time series is anomalous. In addition, comparison of detrended time series from stations along the east coast of Honshu does not reveal along-strike (N-S) propagation of the transient (Figure 2). An updip migration of deep aseismic slip that is laterally extensive along the strike of the plate interface—as in Figure 5—would be consistent with this observation.

The GPS observations are consistent with a combination of updip migration of the transition depth and increasing slip rate above this depth. The downdip limit of seismicity on the Japan trench is around 60 km [Igarashi *et al.*, 2001], with large ($M_w \sim 7$) events occurring in the depth range ~30 to 50 km. High-frequency radiation during the 2011 $M_w 9$ Tohoku earthquake came from ~60 km depth [Meng *et al.*, 2011]; afterslip following the event has been inferred to extend to ~80 km depth [Ozawa *et al.*, 2012; Johnson *et al.*, 2012], suggesting primarily aseismic slip below ~60 km. The simple 2-D model suggests a decrease in transition depth, with an 84% probability of the transition depth in 2011 being deeper than the downdip limit of seismicity (Figure 5b). The GPS data alone allow a wide range of solutions. The most likely solution predicts that a large part of the megathrust accelerated to 65 mm/yr, i.e., only ~20% locked, in depths below 22 km, with only a small decrease in the transition depth (Figures 5b and 5c). (We note that the average slip rate presumably results from a combination of locked asperities and surrounding creep.) However, there are also candidate solutions in which the transition depth shallows to roughly 50 km, with a much more modest increase in slip rate from 50 to 22 km depth. Additional constraints will be needed to discriminate between such end-member models.

5. Conclusion

We have documented regionally coherent and statistically significant decadal-scale interseismic crustal accelerations in northeastern Japan preceding the $M_w 9.0$ 2011 Tohoku-oki earthquake. While the acceleration field in northern Tohoku (Sanriku area) can be explained by postseismic deformation from large earthquakes before 1996, the acceleration field in central and southern Tohoku appears to be unrelated to postseismic effects, of either $M_w \geq 6.3$ events in the period 1996 to 2011, or $M_w \geq 7.5$ events in the period 1938 to 1996. The acceleration field can be explained by increasing slip rate on the Japan trench plate interface and/or updip migration of deep aseismic slip in the decades before the 2011 Tohoku-oki earthquake.

Acknowledgments

We thank the Geospatial Information Authority of Japan and Shin'ichi Miyazaki for providing GPS data, Angelyn Moore for helpful discussions concerning data processing, Yo Fukushima for providing source parameters for the viscoelastic modeling, and Andrew Bradley for assisting with computations. Support was provided by National Science Foundation award EAR-1141931 and a Stanford Graduate Fellowship to A.P.M. We thank J.C. Savage and an anonymous reviewer for their constructive comments. Data are available from http://datahouse1.gsi.go.jp/terras/terras_english.html or upon request from the authors.

The Editor thanks James Savage and an anonymous reviewer for their assistance in evaluating this paper.

References

- Anderson, G., D. C. Agnew, and H. O. Johnson (2003), Salton Trough regional deformation estimated from combined trilateration and survey-mode GPS data, *Bull. Seismol. Soc. Am.*, 93(6), 2402–2414.
Baba, T., A. Ito, Y. Kaneda, T. Hayakawa, and T. Furumura (2006), 3-D seismic wave velocity structures in the Nankai and Japan Trench subduction zones derived from marine seismic surveys, *Abstract of the Meeting of Japan Geoscience Union*.
DeMets, C., R. G. Gordon, and D. F. Argus (2010), Geologically current plate motions, *Geophys. J. Int.*, 181(1), 1–80.
Fukuda, J., A. Kato, N. Kato, and Y. Aoki (2013), Are the frictional properties of creeping faults persistent? Evidence from rapid afterslip following the 2011 Tohoku-oki earthquake, *Geophys. Res. Lett.*, 40, 3613–3617, doi:10.1002/grl.50713.
Geospatial Information Authority of Japan (2011), Estimated slip deficit distribution in northeast and southwest Japan [in Japanese with English figure captions], *Report of Coordinating Committee for Earthquake Prediction*, 86, 226.
Hashimoto, C., A. Noda, T. Sagiya, and M. Matsuzura (2009), Interplate seismogenic zones along the Kuril-Japan trench inferred from GPS data inversion, *Nat. Geosci.*, 2(2), 141–144.
Hashimoto, M. (1990), Horizontal strain rates in the Japanese islands during interseismic period deduced from geodetic surveys (Part I): Honshu, Shikoku and Kyushu [in Japanese with English abstract and figure captions], *J. Seismol. Soc. Jpn.*, 43, 13–26.
Hearn, E., F. Pollitz, W. Thatcher, and C. Onishi (2013), How do “ghost transients” from past earthquakes affect GPS slip rate estimates on southern California faults?, *Geochem. Geophys. Geosyst.*, 14, 828–838, doi:10.1002/ggge.20080.
Heki, K., and Y. Mitsui (2013), Accelerated pacific plate subduction following interplate thrust earthquakes at the Japan trench, *Earth Planet. Sci. Lett.*, 363, 44–49.
Hooper, A., J. Pietrzak, W. Simons, H. Cui, R. Riva, M. Naeije, A. Terwisscha van Scheltinga, E. Schrama, G. Stelling, and A. Socquet (2013), Importance of horizontal seafloor motion on tsunami height for the 2011 $M_w = 9.0$ Tohoku-Oki earthquake, *Earth Planet. Sci. Lett.*, 361, 469–479.

- Igarashi, T., T. Matsuzawa, N. Umino, and A. Hasegawa (2001), Spatial distribution of focal mechanisms for interplate and intraplate earthquakes associated with the subducting Pacific plate beneath the northeastern Japan arc: A triple-planed deep seismic zone, *J. Geophys. Res.*, 106(B2), 2177–2191.
- Ishikawa, N., T. Tada, and M. Hashimoto (1998), Horizontal strain in Japanese islands, *J. Geog. Surv. Inst.*, 89, 18–26.
- Johnson, K. M., J. Fukuda, and P. Segall (2012), Challenging the rate-state asperity model: Afterslip following the 2011 M9 Tohoku-oki, Japan, earthquake, *Geophys. Res. Lett.*, 39, L20302, doi:10.1029/2012GL052901.
- Langbein, J. (2004), Noise in two-color electronic distance meter measurements revisited, *J. Geophys. Res.*, 109, B04406, doi:10.1029/2003JB002819.
- Loveless, J. P., and B. J. Meade (2010), Geodetic imaging of plate motions, slip rates, and partitioning of deformation in Japan, *J. Geophys. Res.*, 115, B02410, doi:10.1029/2008JB006248.
- Loveless, J. P., and B. J. Meade (2011), Spatial correlation of interseismic coupling and coseismic rupture extent of the 2011 $M_W = 9.0$ Tohoku-oki earthquake, *Geophys. Res. Lett.*, 38, L17306, doi:10.1029/2011GL048561.
- Meng, L., A. Inbal, and J.-P. Ampuero (2011), A window into the complexity of the dynamic rupture of the 2011 Mw 9 Tohoku-Oki earthquake, *Geophys. Res. Lett.*, 38, L00G07, doi:10.1029/2011GL048118.
- Nakagawa, H., et al. (2009), Development and validation of GEONET new analysis strategy (Version 4) [in Japanese], *J. Geogr. Surv. Inst.*, 118, 1–8.
- Nishimura, T. (2012), Crustal deformation of northeastern Japan based on geodetic data for recent 120 years [in Japanese with English abstract and figure captions], *J. Geol. Soc. Jpn.*, 118(5), 278–293.
- Nishimura, T., T. Hirasawa, S. Miyazaki, T. Sagiya, T. Tada, S. Miura, and K. Tanaka (2004), Temporal change of interplate coupling in northeastern Japan during 1995–2002 estimated from continuous GPS observations, *Geophys. J. Int.*, 157(2), 901–916.
- Ozawa, S., T. Nishimura, H. Munekane, H. Suito, T. Kobayashi, M. Tobita, and T. Imakiire (2012), Preceding, coseismic, and postseismic slips of the 2011 Tohoku earthquake, Japan, *J. Geophys. Res.*, 117, B07404, doi:10.1029/2011JB009120.
- Peng, Z., and J. Gomberg (2010), An integrated perspective of the continuum between earthquakes and slow-slip phenomena, *Nat. Geosci.*, 3(9), 599–607.
- Perfettini, H., and J.-P. Avouac (2004), Postseismic relaxation driven by brittle creep: A possible mechanism to reconcile geodetic measurements and the decay rate of aftershocks, application to the Chi-Chi earthquake, Taiwan, *J. Geophys. Res.*, 109, B02304, doi:10.1029/2003JB002488.
- Rolandone, F., R. Bürgmann, D. Agnew, I. Johanson, D. Templeton, M. d'Alessio, S. Titus, C. DeMets, and B. Tikoff (2008), Aseismic slip and fault-normal strain along the central creeping section of the San Andreas fault, *Geophys. Res. Lett.*, 35, L14305, doi:10.1029/2008GL034437.
- Suito, H., T. Nishimura, M. Tobita, T. Imakiire, and S. Ozawa (2011), Interplate fault slip along the Japan Trench before the occurrence of the 2011 off the Pacific coast of Tohoku Earthquake as inferred from GPS data, *Earth Planets Space*, 63(7), 615–619.
- Thatcher, W. (1983), Nonlinear strain buildup and the earthquake cycle on the San Andreas fault, *J. Geophys. Res.*, 88(B7), 5893–5902.
- Ueda, H., M. Ohtake, and H. Sato (2003), Postseismic crustal deformation following the 1993 Hokkaido Nansei-oki earthquake, northern Japan: Evidence for a low-viscosity zone in the uppermost mantle, *J. Geophys. Res.*, 108(B3), 2151, doi:10.1029/2002JB002067.